

Characterization of extended defects of ZnTe/GaAs(100) hetero-interface by advanced transmission electron microscopy

This article has been downloaded from IOPscience. Please scroll down to see the full text article.

2002 J. Phys.: Condens. Matter 14 13305

(<http://iopscience.iop.org/0953-8984/14/48/382>)

View [the table of contents for this issue](#), or go to the [journal homepage](#) for more

Download details:

IP Address: 171.66.16.97

The article was downloaded on 18/05/2010 at 19:17

Please note that [terms and conditions apply](#).

Characterization of extended defects of ZnTe/GaAs(100) hetero-interface by advanced transmission electron microscopy

D Shindo¹, Y-G Park, B J Kim, J F Wang and M Isshiki

Institute of Multidisciplinary Research for Advanced Materials, Tohoku University, 1-1 Katahira, 2-Chome, Aobaku, Sendai 980-8577, Japan

E-mail: shindo@tagen.tohoku.ac.jp

Received 27 September 2002

Published 22 November 2002

Online at stacks.iop.org/JPhysCM/14/13305

Abstract

The microstructure of a wide gap ZnTe epilayer on a (100) GaAs substrate has been investigated in detail by transmission electron microscopy (TEM). Through high-resolution electron microscopy (HREM), extended defects such as dislocations and stacking faults have been clearly observed in the ZnTe epilayer near the interface. Considerable lattice misorientation in the local area of the epilayer was clarified, being consistent with the results of x-ray diffraction. Furthermore, it was found that the lattice contraction along the [200] direction and the lattice expansion along the $[0\bar{2}2]$ direction exist in the GaAs substrate. The lattice contraction and expansion were quantitatively analysed by advanced TEM, i.e., image analysis on HREM images and nano-beam electron diffraction.

1. Introduction

For II–VI epilayers, III–V substrates have been utilized, since II–VI substrates of high quality for homoepitaxy are difficult to obtain. In fact, wide gap II–VI materials such as ZnTe and ZnSe have been extensively grown on III–V substrates of GaAs and GaSb. It has been reported that the quality of the II–VI epilayers is directly influenced by the lattice mismatch and the difference in thermal expansion coefficients between the epilayer and the substrate, in addition to the impurity diffusion from the substrate [1–3]. Recently, ZnTe film has attracted much attention, since it has a direct bandgap of 2.26 eV at room temperature and has a potential in use for green light emitting devices [4]. In the ZnTe/GaAs heterostructure system, there exists large strain resulting from the large lattice mismatch of about 8% and the difference in thermal expansion coefficients between ZnTe and GaAs. It was reported that the high density of the

¹ Author to whom any correspondence should be addressed.

dislocations was generated in the epilayer to relax the strain, resulting in the degradation of optical properties of the epilayer [1, 3, 5, 6].

In order to understand the structural and optical properties of the semiconductors of the heterostructure system in detail, it is generally most important to precisely characterize the microstructures of both epilayer and substrate. So far, much attention has been focused on the nature of the misfit dislocations at the hetero-interface and on the density of the extended dislocations in the epilayer [3, 7, 8]. In this paper, extended defects at the hetero-interface and in both the epilayer and the substrate in the ZnTe/GaAs system were observed by using conventional transmission electron microscopy (TEM) and high-resolution electron microscopy (HREM). Furthermore, the lattice strain around the hetero-interface was quantitatively analysed by advanced TEM, i.e., image analysis on HREM images and nano-beam electron diffraction.

2. Experimental procedure

ZnTe films were grown on (100) GaAs substrates by hot wall epitaxy (HWE), which could be carried out under near thermal-equilibrium condition at all the steps by installing a hot wall between the source and the substrate. The detailed setup and epitaxial conditions of the HWE have been described elsewhere [9].

The high resolution four-crystal x-ray diffraction (XRD) was measured with a Rigaku SLX-2000 having a 10 kW Cu radiation source. The x-ray beam from a Cu tube was monochromatized by the four reflections of a Bartels monochromator at the (220) face of perfect channel-cut germanium single crystals. Thin foils for TEM studies were prepared by conventional techniques, including mechanical polishing, dimpling and thinning with a low energy (2.5 keV) Ar ion-beam at a 13° inclination. The detailed study of the defects and hetero-interface was carried out through cross-sectional HREM observation using a JEM-ARM 1250 TEM with the accelerating voltage of 1250 kV, which has a theoretical point-to-point resolution of 0.1 nm. On the other hand, a JEM-3000F TEM installed with a field emission gun was used for the nano-beam electron diffraction study with a probe size of about 7 nm.

3. Results and discussion

Figures 1(a) and (b) show the rocking curves of $\omega-2\theta$ and ω scans for the 400 reflection of the ZnTe epilayers of 0.7 and 12 μm in thickness; hereafter we indicate these specimens as ZnTe (0.7 μm)/GaAs and ZnTe (12 μm)/GaAs, respectively. In (a) and (b), it is found that the difference of the full width at half maximum (FWHM) between $\omega-2\theta$ and ω scans in the ZnTe (0.7 μm) is 5.5 times, while that in the ZnTe (12 μm) is 3.5 times. It is considered that the quality of the epilayer in ZnTe (12 μm)/GaAs is much better than that of ZnTe (0.7 μm)/GaAs. Furthermore, it is noted that the value (66 arc s) of the FWHM in (b) is the best value so far reported to our knowledge, and the high quality of the ZnTe epilayer was confirmed by photoluminescence and reflection spectra in our co-workers' paper [9].

Figures 2(a) and (b) show typical bright-field cross-sectional images in the ZnTe (0.7 μm)/GaAs and ZnTe (12 μm)/GaAs, respectively. The images were observed under the two-beam diffraction condition with the reflection ($g = 0\bar{2}2$) excited. In both cases, there are a lot of dislocations in the epilayer, especially near the hetero-interface. It is noted that the dislocation density becomes lower by increasing the distance from the interface. The result obtained from XRD for characterizing the quality of the epilayer in figure 1 is consistent with this TEM observation. In the following, the detailed microstructure in the ZnTe (12 μm)/GaAs system is further analysed by TEM.

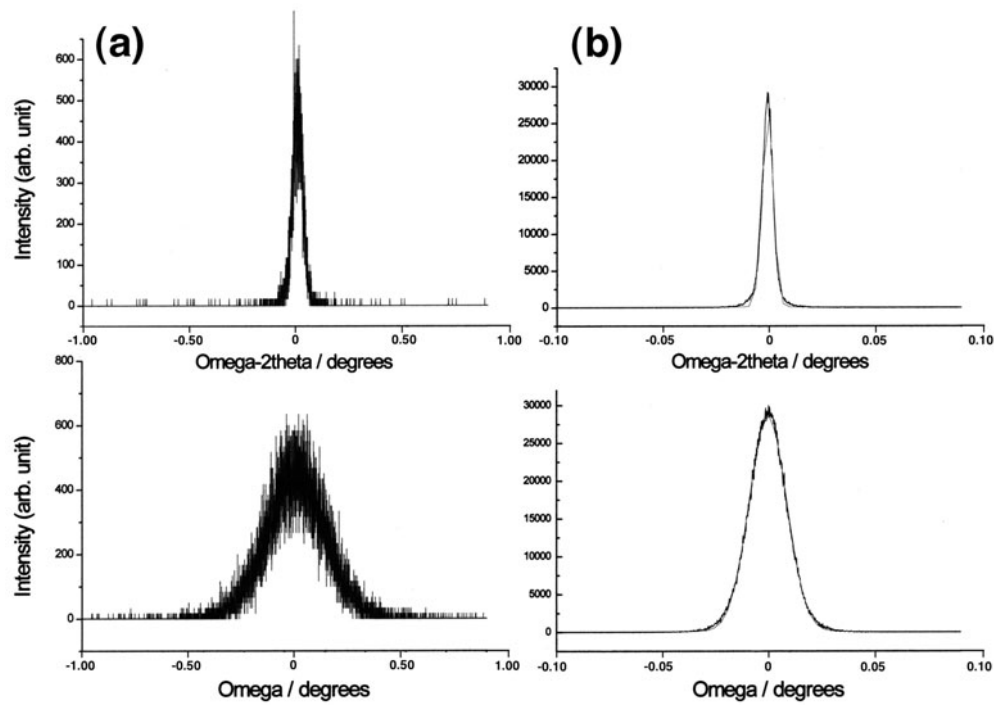


Figure 1. Rocking curves of $\omega-2\theta$ (upper part) and ω (lower part) scans on a ZnTe epilayer of $0.7\ \mu\text{m}$ (a) and $12\ \mu\text{m}$ (b) in thickness. FWHMs of the rocking curves for $\omega-2\theta$ and ω scans in (a) are evaluated to be 237 and 1295 arc s, respectively. FWHMs in those of (b) are 19 and 66 arc s.

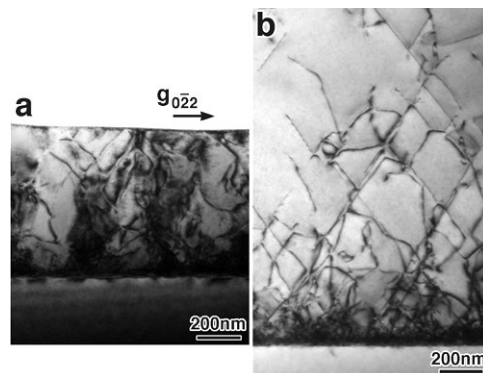


Figure 2. Bright-field images of ZnTe ($0.7\ \mu\text{m}$)/GaAs (a) and ZnTe ($12\ \mu\text{m}$)/GaAs (b) taken under the two-beam diffraction condition with the reflection ($g = 022$) excited.

Figure 3 shows a (011) cross-sectional HREM image of the system with the incident electron beam parallel to the [011] direction. It is seen that there is a bright region along the hetero-interface. This image contrast is considered to result from the strong lattice strain. The lattice fringes of ZnTe and GaAs connect at the interface in some areas, while some discontinuity of the lattice fringes is observed as indicated by arrows. The discontinuity is considered to result from the large mismatch between ZnTe and GaAs lattices. Apparently, there may exist misfit dislocations at the interface.

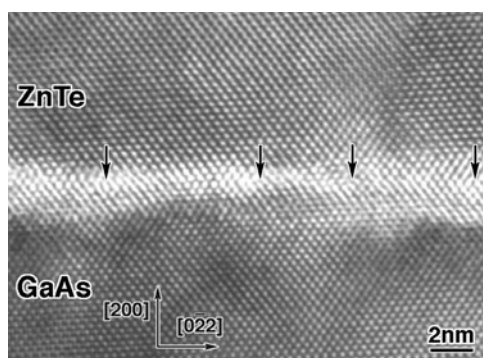


Figure 3. Cross-sectional HREM image of ZnTe ($12\ \mu\text{m}$)/GaAs obtained with the incident electron beam parallel to the $[011]$ direction.

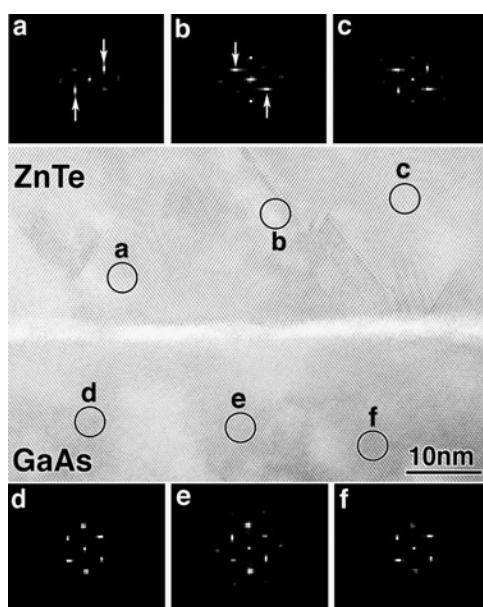


Figure 4. Cross-sectional HREM image showing relatively wide area. The digital diffractograms (a)–(f) obtained from the circle regions (a–f) in the HREM image.

Figure 4 shows an HREM image of relatively wide area around the hetero-interface in the ZnTe ($12\ \mu\text{m}$)/GaAs system. In order to investigate the lattice misorientation, three digital diffractograms were obtained from both of the ZnTe epilayer and GaAs substrate. While the excited reflections indicated by arrows change from place to place in the ZnTe epilayer, relatively speaking no drastic misorientation is observed in the digital diffractogram of the GaAs substrate. The large misorientation observed in the ZnTe epilayer is considered to result from the considerable strain field around the partial dislocations at the end of stacking faults. Taking into account the relatively small lattice misorientation in the GaAs substrate, the lattice spacing in the GaAs substrate near the interface was measured through the digital diffractogram as shown in figure 6.

Figure 5 shows a bright-field image, a conventional electron diffraction pattern and nano-beam diffraction patterns of the ZnTe ($12\ \mu\text{m}$)/GaAs system. The conventional electron

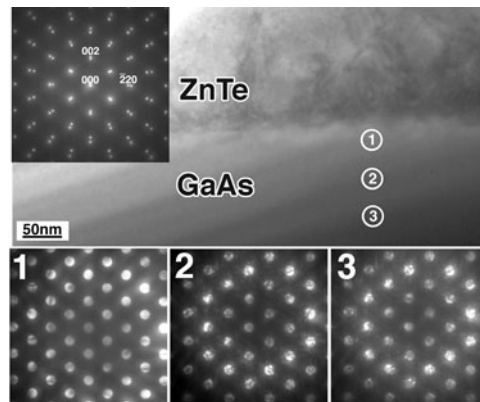


Figure 5. Bright-field image and a conventional electron diffraction obtained from ZnTe ($12 \mu\text{m}$)/GaAs. Nano-beam diffraction patterns (1–3) were obtained from the circle regions (1–3) in the bright-field image.

diffraction pattern was obtained from a wide area including the hetero-interface with a selected area aperture of a diameter $1.3 \mu\text{m}$. It is clearly seen that two kinds of diffraction pattern corresponding to ZnTe ($d_{200} = 0.3051 \text{ nm}$, $d_{0\bar{2}2} = 0.2159 \text{ nm}$) and GaAs ($d_{200} = 0.2825 \text{ nm}$, $d_{0\bar{2}2} = 0.1998 \text{ nm}$) overlap. Nano-beam diffraction patterns were observed from three regions indicated in the figure. It is interesting to note that a nano-beam diffraction pattern obtained from the region (1) near the interface has no definite fine structure in the nano-beam diffraction discs, while the other discs obtained at distances more than 60 nm from the interface contain fine structure with dark lines. The result clearly indicates that the lattice strain becomes smaller with the increase of the distance from the interface. From the spacings of the nano-beam diffraction discs, the lattice spacing of the GaAs substrate was measured as shown in figure 6. Diamonds and open circles in (a) and (b) correspond to the lattice spacings measured from nano-beam diffraction and the digital diffractogram of the HREM image, respectively. In the lower right parts in both figures 6(a) and (b), the error bars for the accuracy in measuring the lattice spacing by nano-beam diffraction and the HREM image are presented. Dispersion of the data over the error bars is considered to result from inhomogeneous distribution of lattice strain, and especially the considerable dispersion of some data obtained from the HREM image in figure 6(a) is considered to be sensitively affected by the localized lattice strain which can be seen in figure 4. Nevertheless, it is seen that the result of nano-beam diffraction is consistent with the result obtained from the digital diffractogram of the HREM image. The solid lines in (a) and (b) indicate the interplanar spacing of the (200) and ($0\bar{2}2$) planes in bulk GaAs. As indicated by dotted lines, appreciable lattice strain is observable at least at the distance 150 nm from the interface. It is interesting to note that there is lattice contraction and expansion along the vertical and the horizontal directions which correspond to the [200] and [$0\bar{2}2$] directions, respectively. Furthermore, it is found that 0.35% of lattice contraction and 0.44% of lattice expansion exist at a distance of 20 nm from the interface. One of the possible causes for the existence of the lattice contraction and expansion in the GaAs substrate is considered as follows. While the ZnTe film is grown at high temperature, the mismatch at the interface between ZnTe and GaAs is partly accommodated by the introduction of dislocations as observed in figures 2(a) and (b). On the other hand, when the temperature of the film comes down to room temperature, due to the different thermal expansion coefficients α of ZnTe and GaAs ($\alpha_{\text{ZnTe}} = 8.3 \times 10^{-6} \text{ K}^{-1}$, $\alpha_{\text{GaAs}} = 6.86 \times 10^{-6} \text{ K}^{-1}$), the film tends to have some

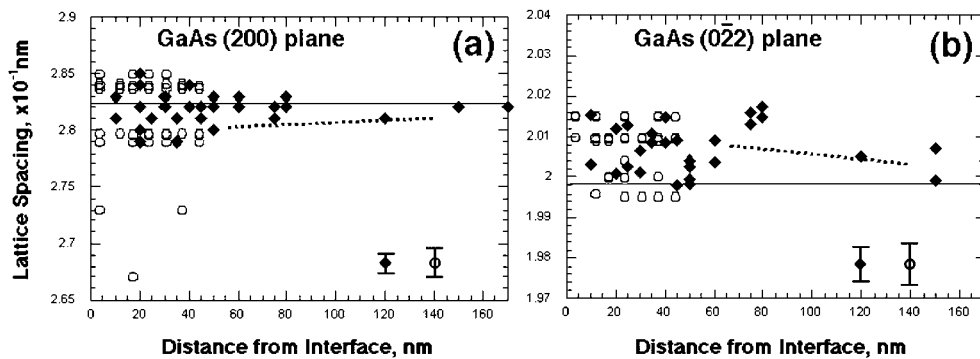


Figure 6. Lattice spacings of the (200) plane (a) and $(0\bar{2}2)$ plane (b) measured by nano-beam diffraction (\blacklozenge) and digital diffractogram (\circ) of the GaAs substrate in ZnTe (12 μm)/GaAs. Error bars are indicated in the lower right parts of both figures.

curvature resulting in contraction in the ZnTe layer and expansion in the GaAs substrate along the $[0\bar{2}2]$ direction. Also, expansion along the $[0\bar{2}2]$ direction inevitably produces contraction along the $[200]$ direction in the GaAs substrate, keeping its volume unchanged.

Finally, it is noted that the combination of analysis of HREM images and nano-beam diffraction will give quantitative information about lattice strain around the interface of a heterostructure such as the ZnTe/GaAs system.

4. Conclusions

The results obtained by HREM and nano-beam diffraction study on a ZnTe/GaAs(100) thin film with an epilayer thickness of 12 μm prepared by HWE are summarized as follows.

- (1) The extended dislocations and stacking faults in the ZnTe epilayer were clearly observed by HREM. The density of dislocations becomes lower with increase of the distance from the hetero-interface.
- (2) Due to the strain field of partial dislocations, considerable lattice misorientation was observed in the ZnTe epilayer, especially near the hetero-interface.
- (3) In the GaAs substrate, there exist lattice contraction along the vertical direction ($[200]$ direction) and lattice expansion along the horizontal direction ($[0\bar{2}2]$ direction). The percentages of the lattice contraction and expansion of GaAs substrate at a distance of 20 nm from the interface were evaluated to be 0.35 and 0.44%, respectively.
- (4) Considerable lattice strain in the GaAs substrate was found to extend to a distance of 150 nm from the interface.

References

- [1] Kudlek G, Presser N, Gutowski J, Hingerl K, Abram E, Pesek A, Pauli H and Sitter H 1992 *J. Cryst. Growth* **117** 290
- [2] Petruzzello J, Olego D J, Chu X and Faurie J P 1988 *J. Appl. Phys.* **63** 1783
- [3] Zhang Y, Skromme B J and Turco-Sandroff F S 1992 *Phys. Rev. B* **46** 3872
- [4] Han J, Stavrinides S, Kobayashi M, Gunshor R L, Hagerott M M and Nurmikko A V 1993 *Appl. Phys. Lett.* **62** 840
- [5] Kim B J, Wang J F, Ishikawa Y, Park Y-G, Shindo D, Abe S, Masumoto K and Isshiki M 2002 *J. Cryst. Growth* **235** 201

-
- [6] Leiderer H, Jahn G, Silberbauer M, Kuhn W, Wagner H P, Limmer W and Gebhardt W 1991 *J. Appl. Phys.* **70** 398
 - [7] Bauer S, Rosenauer A, Skorsetz J, Kuhn W, Wagner H P, Zweck J and Gebhardt W 1992 *J. Cryst. Growth* **117** 297
 - [8] Clifton P A, Mullins J T, Brown P D, Russell G J, Brinkman A W and Woods J 1988 *J. Cryst. Growth* **93** 726
 - [9] Kim B J, Wang J F, Ishikawa Y, Sato S and Isshiki M 2002 *Phys. Status Solidi a* **191** 161